PCCP

Accepted Manuscript


This is an *Accepted Manuscript*, which has been through the Royal Society of Chemistry peer review process and has been accepted for publication.

*Accepted Manuscripts* are published online shortly after acceptance, before technical editing, formatting and proof reading. Using this free service, authors can make their results available to the community, in citable form, before we publish the edited article. We will replace this *Accepted Manuscript* with the edited and formatted *Advance Article* as soon as it is available.

You can find more information about *Accepted Manuscripts* in the Information for Authors.

Please note that technical editing may introduce minor changes to the text and/or graphics, which may alter content. The journal's standard Terms & Conditions and the Ethical guidelines still apply. In no event shall the Royal Society of Chemistry be held responsible for any errors or omissions in this *Accepted Manuscript* or any consequences arising from the use of any information it contains.

ROYAL SOCIETY OF CHEMISTRY

www.rsc.org/pccp

Physical Chemistry Chemical Physics
CREATED USING THE RSC LaTeX PCCP ARTICLE TEMPLATE – SEE www.rsc.org/electronicfiles FOR DETAILS
ARTICLE TYPE www. rsc.org/xxxxxx | XXXXXXXX

# Do bifunctional labels solve the problem of dye diffusion in FRET analysis?†

**Katarzyna Walczewska-Szewc*[ab] and Ben Corry*[a]**

***Received Xth XXXXXXXXXX 200X, Accepted Xth XXXXXXXXX 20XX***
***First published on the web Xth XXXXXXXXXX 200X***
**DOI: 10.1039/b000000x**

We examine the potential application of bifunctional dyes in Förster resonance energy transfer (FRET) experiments due to their increasing popularity in electron paramagnetic resonance spectroscopy. To do this we conduct molecular simulations of the well characterised all-*trans* polyproline labelled with both mono- and bifunctional rosamine dyes to understand the influence of bifunctionalisation on dye diffusion, orientation and transfer efficiency. As there is a more stiff connection between the labels and the host molecule, the effect of dye diffusion is significantly reduced with bifunctional labels when compared to traditional labels, yielding a narrower FRET efficiency distribution and overcoming a serious hurdle in FRET data analysis. However, the more restricted motion of the bifunctional dyes limits the relative orientation of the dyes, taking the system away from the commonly assumed approximation of isotropic dye orientations. While bifunctional dyes may make it easier to distinguish conformational or biochemical states of the system, they may make it harder to relate transfer efficiencies to distances if the dye orientations are not known.

## 1 Introduction

The use of bifunctional spin labels is increasingly popular technique in electron paramagnetic resonance (EPR) spectroscopy [1–4], allowing for significantly reduced movement of the label with respect to the host molecule. Thus, more accurate and precise distance determination between two labels is possible. Given the promising results of EPR studies that show an improvement in the quality of distance measurements, we would like to test if bifunctional dyes would be useful in Förster Resonance Energy Transfer (FRET) studies. FRET in combination with single molecule (SM) spectroscopy is a powerful technique that can be used to identify the motion and structural changes in molecules, such as protein folding or conformational change during the function of proteins [5–8]. In this kind of non radiative transfer, the quantum of energy is passed from an excited state molecule called the donor to a ground state molecule called the acceptor via coulombic interactions. Thus, FRET can be detected by selectively exciting the donor and observing how often the energy is transferred to the acceptor instead of being spontaneously emitted. The dependency of the transfer efficiency on the dye to dye distance, $R$, can be described via Förster theory, which joins the quantum mechanical formalism of electromagnetic coupling with the spectroscopic properties of the dyes. Hence, the efficiency of transfer is given by

$$E = \frac{R_0^6}{R_0^6 + R^6} \tag{1}$$

where $R_0$ is the so called Förster radius determining the distance at which FRET and donor fluorescence are equally probable [9],

$$R_0^6 = 8.79 \times 10^{-5} \cdot \frac{\kappa^2 \Phi_D}{n^4} \cdot J \tag{2}$$

In this, $n$ is the refractive index, $\Phi_D$ is the quantum yield of the donor in the absence of acceptor, $J$ is the spectral overlap of the pair of fluorophores and $\kappa^2$ describes the relative orientation of the donor and acceptor transition dipoles which can be defined as

$$\kappa^2 = (\cos\theta_T - 3\cos\theta_D \cos\theta_A)^2 \tag{3}$$

Here, $\theta_T$ is the angle formed by donor and acceptor transition moments, $\theta_D$ and $\theta_A$ are the angles between each transition moments and the vector joining the middle point of each dipole. The influence of $\kappa^2$ is usually neglected in distance determination, since in the case of fast, unrestrained and uncorrelated rotation of fluorophores, the so called isotropic approximation can be used and the constant value of $\kappa^2 = 2/3$ can be assumed [9]. Nevertheless the presence of steric obstacles provided by the structure of a host molecule or the dye linker can disturb the free rotation and, if the isotropic assumption is no longer valid, the orientation factor can vary in the range of

† Electronic Supplementary Information (ESI) available: [details of any supplementary information available should be included here]. See DOI: 10.1039/b000000x/

[a] *Research School of Biology, Australian National University, Australia. E-mail: fizkws@ug.edu.pl (for KWS), ben.corry@anu.edu.au (for BC)*
[b] *Institute of Experimental Physics, University of Gdansk, Poland.*



Physical Chemistry Chemical Physics Accepted Manuscript

0 to 4. In most situations, direct measurements of the dye orientations are not possible [10–13]. Applying bifunctional FRET labels to protein systems might potentially reduce the effect of orientation changes by restraining the dyes rotation with respect to the host molecule.

The next problem which potentially could be addressed using bifunctional dyes arises due to relative mobility of commonly used fluorescent labels with respect to the macromolecule to which they are attached. Depending on the length of the linker, this can introduce a significant uncertainty in distance determination. What is more, the FRET measurements relate to the separation of the fluorescent labels, which may differ from the distance between the residues to which the dyes are attached. Because of cross-linking with the macromolecule, bifunctional probes minimize the relative motion of the fluorescent label, which has been experimentally confirmed in EPR spectroscopy studies [1,2]. In those, more precise distances have been obtained in comparison with the traditional spin labels which are characterized by high conformational flexibility and cause a significant broadening of distance distribution.

The use of bifunctional versions of fluorescent dyes has not yet been established in FRET spectroscopy, however the first bifunctional fluorescent labels have been synthesised [14,15]. Using well embedded bifunctional dyes in the case of FRET measurements can have two positive effects. First, the dye is almost immobilised, which reduces the influence of dye diffusion. Second, its orientation relative to the host is restrained and the average value of the orientation factor can be, in some situations, assessed. Such control on the fluorophores orientation might potentially be used to increase the range of FRET for use as a spectroscopic ruler.

Here we performed a simulation study of a simple system of dyes attached to polyproline in order to see the influence of bifunctionalisation on the FRET distribution. Three cases of dye tethering are analysed: a bifunctional dye and monofunctional dyes with short and long linker.

## 2 Methods

To analyse the influence of the linker type on the amount of dye diffusion, three fluorescent dyes were examined. Two maleimide derivatives of Rosamine (Fig. 1a,b) characterised by different length of the linker are tethered to cysteine residues via chemical conjugation of a maleimide group to a sulfhydryl. Third, a bifunctional dye [15] (Fig 1c), is attached to a protein by two reactions between iodoacetamide groups and cysteines.

We decided to examine rosamine based dyes, whose spectral properties have been well examined over last years [16,17]. The bifunctional form of rosamine was first synthesised by Hirayana et a.l in 2007. One of the advantages of using this kind of dye is that rosamine does not have any substituent on a phenyl ring, which eliminates a problem of formation of diastereomers in the bifunctional form, as happens in the case of structurally similar rhodamine [14,15].

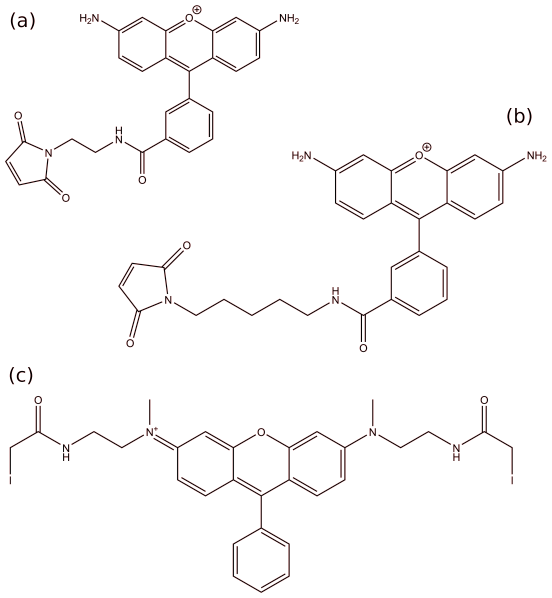


**Fig. 1** The chemical structure of three versions of dye used in our simulations. The short version of maleimide derivative of rosamine (a), the same dye with three additional carbon atoms in the linker (b) and the bifunctional rosamine synthesised by Hirayama et al. [15] (c)

The next step was to build three molecular systems, in which the dyes were tethered to a macromolecule. As a host molecule, the $\alpha$-helix chain of 23 prolines has been chosen. This system has been studied repeatedly over the last years both in experiments and simulations [18–21], and is treated as a standard in FRET experiments. The chain of all *trans* prolines is regarded to be quite rigid [18], however, to be sure that all observed effects result from the dynamics of the attached dyes, and are not influenced by the dynamics of the macromolecule, we restrained the positions of proline $\alpha$ carbons during the MD simulations with a harmonic potential with force constant 1 kcal/mol Å$^2$ (more information in Supplementary Material†). Moreover, all MD frames have been aligned prior to analysis. Depending on the method of dye tethering, different proline residues were replaced with cysteines. In the case of single functional dyes, residues 5 and 19 were changed. To attach bifunctional dyes, four residues: 2, 8, 16, and 22 were mutated, as can be seen in Figure 2.

The MD simulations of three molecular systems were carried out with the NAMD Molecular Dynamic Software version 2.9 [22] using previously developed parameters based on the CHARMM27 force field [23,24] and QM calculations conducted


This journal is © The Royal Society of Chemistry [year]

Physical Chemistry Chemical Physics Accepted Manuscript

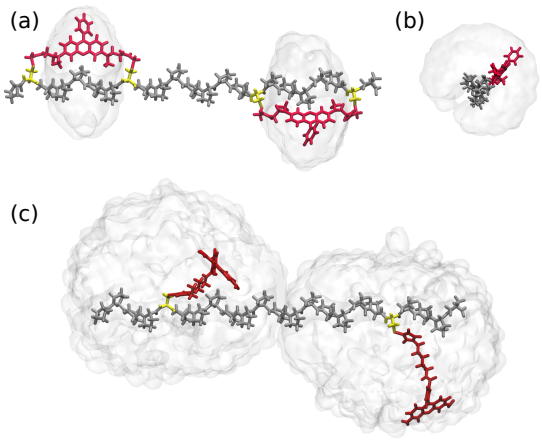


**Fig. 2** Two of the molecular systems used in our simulations. The polyproline chain labelled with bifunctional version of rosamines in front (a) and side view (b) and the long linker monofunctional version (c). Proline residues are coulored grey, cysteines yellow and dyes red. The grey volume around each dye indicates the area sampled by the dye headgroup during the simulation.

using Gaussian[25]. Because our aim was to compare the effect of dye diffusion for three different linker types, without the necessity of obtaining rigorous agreement with an experiment, we decided to proceed simulations in the Generalized Born Implicit Solvent approximation[26,27]. The standard value of dielectric of the solvent (78.5) was used and the concentration of ions in solvent was set to 0.3 M. We applied periodic boundary condition in three dimensions, to avoid the influence of edges on our system. The simulations were performed with constant temperature 298 K maintained using Langevin dynamics and constant pressure of 1 atm maintained using a modified Nosé-Hoover method in which Langevin dynamics is used to control fluctuations in the barostat. All simulations began with an initial minimization period of 1000 steps and were repeated to ensure reproducibility of the results. The total length of each simulation was 1 $\mu$s, which was shown to be sufficient to gain good convergence of the results (see Supplementary Material†).

## 3 Results and Discussion

As expected, the amount of dye diffusion is significantly less for the bifunctional dyes than for the monofunctional versions (grey volumes in Fig. 2). Hence, the distribution of dye-dye distances is much narrower (Fig. 3a, black solid line). The dyes have only a small deviation away from the tethering point (magenta vertical line) which, if the macromolecule dynamics can be neglected, results in very narrow dye-dye distance distribution with the average dye separation very close to the distance between the tethering points. In the case of single linker dyes, the amount of dye diffusion increases with the linker length. For the shorter version of rosamine (Fig. 1a) deviations in position from the point in which it is tethered can reach 20 Å (Fig. 3a, cyan dashed line), whereas adding three carbon atoms to the linker (Fig. 1b) increases the maximum dye diffusion range to 25 Å (Fig. 3a, black dashed line).

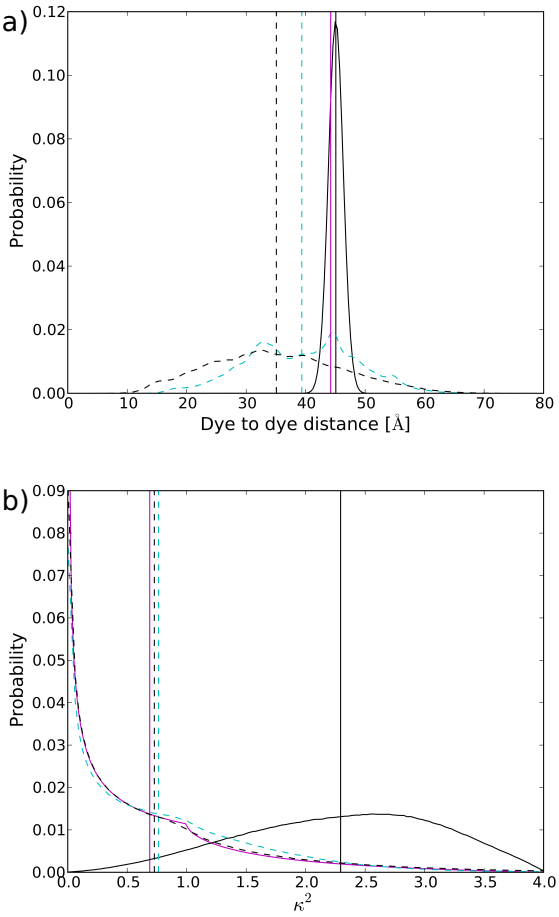


**Fig. 3** Distance and $\kappa^2$ distributions obtained during MD simulation. Dye-dye separation (a) and $\kappa^2$ (b) for three different molecular systems: polyproline labelled with bifunctional dyes (black solid line), monofunctional dyes with short (cyan dashed line) and long linker (black dashed line). The vertical lines indicates the average values of the distributions with the same colour. Solid magenta line represents the distance between residues 5 and 19 (a), and the analytical distribution of orientation factor[9] (b).

Having a long, flexible linker is important to ensure free and unrestrained rotation of the transition dipole, which has previously been shown to lie roughly along the plane of the

Physical Chemistry Chemical Physics Accepted Manuscript

aromatic head group of each dye[24]. This condition is necessary to apply the isotropic approximation to the value of the orientation factor, $\kappa^2$. The $\kappa^2$ distribution for shorter (Fig. 3b, cyan dashed line) and longer linker (Fig. 3b, black dashed line) monofunctional dyes are very close to the analytical one expected for unrestrained motion (solid magenta line). Although for short linker there are small deviations from isotropic rotation, the fact that $\langle\kappa^2\rangle \approx 2/3$ suggests that the isotropic condition is still fulfilled. This means that even the shorter linker is long enough to prevent the steric clashes with the proline chain.

The situation is different when the dye is tethered to the protein chain using two linker groups. The rotation of the dye is strongly restrained and, due to the stiff connection between dye and macromolecule, reflects the changes in orientation of the protein to which it is attached. In our case with an immobilized protein, the value of the orientation factor oscillates around the mean value, which is determined by how the dyes are attached during system construction (Fig. 3b, black solid line). In this case $\langle\kappa^2\rangle = 2.3$ which clearly indicates, that the isotropic approximation is no longer valid.

The distribution of FRET efficiencies can be calculated by combining the dye-to-dye distance, $\kappa^2$ distributions and the Föster radius $R_0 = 52.9$ Å for homotransfer between two rosamine dyes. This value was calculated based on the spectroscopic properties of rosamines published by Wu & Burgess in 2008[16] and with assumption that spectral properties of dye are the same for both single and bifunctional form (for more information see Supplementary Material†).

FRET data were calculated in two different averaging regimes[9]. The first set (Fig. 4a) is calculated in the so called static regime, in which the instantaneous value of $\kappa^2$ is assigned to each distance in Eq. 1-3. This kind of averaging is used when dyes change their orientations slowly enough to assume that the energy transfer occurs between dipoles with well defined orientation. An alternative situation is when rotation of fluorescent labels is fast and the entire range of possible orientations are sampled during the transfer time. In this so called dynamic averaging regime (Fig. 4b) the average value of orientation factor should be used. Additionally, to mirror the experimental conditions, in which a recorded signal usually comes from averaging a bunch of several photons, emitted by dyes of different position and orientation, we applied a burst averaging scheme[28,29]. Each data point in Figure 4 is created by averaging five randomly chosen points from the original FRET histograms.

Regardless of the averaging regime, the system labelled with bifunctional dyes is characterized by a very narrow distribution of FRET efficiency (black solid line). In the case of maleimide derivatives of Rosamine with short (cyan dashed line) and long linker (black dashed line) the efficiency distribution is wider and reflects the wide distribution of dye-to-dye distance.

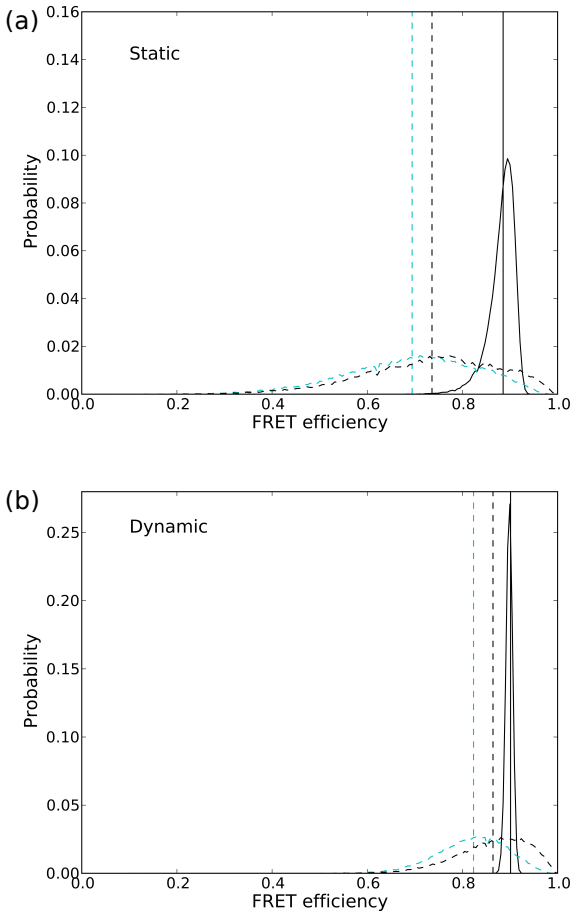


**Fig. 4** The distributions of FRET efficiency obtained in different averaging regimes: static (a) and dynamic (b) for three different molecular systems: polyproline labelled with bifunctionalized dyes (black, solid line), dyes with short (cyan, dashed line) and long linker (black, dashed line). The vertical lines indicates the average values of distributions with the same colour.

Interestingly, the averaging regime influences the distribution of monofunctional dyes much more than bifunctional ones. The average FRET efficiency in static regime are lower by 0.1 in comparison with the dynamic one, while the average values for the bifunctional derivatives remain almost unchanged. The main reason of this effect is the fact that the transfer efficiency changes with orientation factor in a nonlinear manner. Increasing $\kappa^2$ by some value will lead to higher FRET efficiency. However, when decreasing orientation factor by the same value, the observed transfer will be much lower, especially for the dye-to-dye distances near $R_0$. In the case of almost isotropic distribution of $\kappa^2$, as for monofunc-


This journal is © The Royal Society of Chemistry [year]

Physical Chemistry Chemical Physics Accepted Manuscript

tional dyes, this effect is especially visible, due to the shape of the distribution. A majority of $\kappa^2$ values during a simulation will be smaller than the average one, since a high number of 'low' $\kappa^2$ events is required to balance a single 'high' $\kappa^2$ case. That is why the FRET efficiency calculated in the static regime will be lower than in the dynamic one. Analysis of anisotropy decays suggest that the dynamic regime is more appropriate for this system (see Supplementary Information†).

## 4 Conclusions

The advantage of using the bifunctional form of dyes in dealing with a dye diffusion is obvious. The more restraints that are applied to dye motion, the narrower the distribution in dye separation. Hence, the contribution of motion of the dyes themselves to the overall distance distribution is less significant than in the case of standard, single functional dyes. This results in narrow FRET efficiency distributions which may allow for different conformational states of the host to be more easily identified, and to not be confused with different dye positions. Moreover, the geometry of this kind of fluorophore forces a small separation between dye and tethering points so the distance measured between dyes can be directly related to that between the residues that we are interested in. Another possible advantage of using bifunctional dyes is that the dye and protein motion can be easily separated, as the influence of dye diffusion only slightly broadens the distance distribution. For example, if the polyproline chain was not restrained in our simulations, and conformational changes of $\alpha$-helix were allowed, the distance distribution between the two dyes would be significantly broadened. In the case of bifunctional labels almost all broadening could be related directly with protein movement, since the contribution of dye diffusion is almost negligible.

Nevertheless, as opposed to EPR studies, in which the orientation factor is not an issue, in FRET measurements $\kappa^2$ plays very important role. Because the dyes are tethered in two places, the orientation of fluorophores is strongly restrained and the commonly used isotropic approximation, $\kappa^2 = 2/3$, is no longer valid, as the average $\kappa^2$ value can converge to a different value (Fig. 3b). Thus, the data interpretation, especially relating the FRET efficiency to distance, may be problematic, unless the actual value of $\kappa^2$ can be measured. What is more, the geometry of dye tethering may lead to the strong correlation between the orientation factor and the distance. For example, if dyes are tethered to two helices responsible for opening and closing a protein channel, both distance and orientation change during the protein function. This effect is not desirable in FRET measurements if the correlation function is unknown.

One method to overcome this issue might be using bifunctional form of lanthanide dyes, as a FRET donor. This kind of dye contains metals such as europium or terbium and are characterised by isotropic emission. Hence, the average value of $\kappa^2 = 2/3$ could be assumed[30,31]. Nevertheless, the lanthanide dyes are difficult to excite if not linked to special antenna systems[32,33].

On the other hand, the fact that choice of specific labelling sites determines the dye orientation may advantage the transfer efficiency in the case in which the fluorophores are tethered with favourable orientation. The predominantly parallel orientation of dyes, as in our exemplary system, increases the average value of $\kappa^2$ from 0.66 to 2.3 which leads to higher value of FRET efficiency than in the case of freely rotating dyes (Fig. 4b). Thus, the range over which FRET can be used as a spectroscopic ruler can potentially be extended and a measurable level of energy transfer can be achieved for larger distances. Nevertheless, this effect works in both ways and if the average fluorophore orientation is nearly perpendicular, very weak, or even no transfer will occur. Control of fluorophore orientations has previously been obtained by Börjesson et al.[34] for the nucleic acid base analogue FRET-pairs rigidly attached to the DNA strands as well as in study of Lewis et al.[35] in which the fluorophores were positioned at opposite ends of a DNA helix. As a consequence of the donor and acceptor being rigidly located at strategic positions, they could accurately distinguished the distance and orientation changes using FRET.

The fact that the orientation of the fluorophores mirrors the arrangement of residues to which the dyes are attached might be used to measure orientation changes of protein, as long as the distance does not change significantly. Hence, the kinking of helix or relative orientation of two helices could be possibly measured based on changes in FRET efficiency caused by modification of $\kappa^2$.

Another fact, worth mentioning is that during protein dynamics, both dye separation and orientation factor changes can be observed (not only distance, as in the single linker case). Such cross-influence on transfer efficiency in the system labelled with two bifunctional dyes may mean that even very small conformational changes may lead to a FRET change. Hence, the transfer measurements in such systems may be a more sensitive signal to biochemical events than the standard experiment even if it is hard to relate this directly to a change in distance.

In conclusion, although it might seem that the use of bifunctional dyes will be a great advantage in using FRET to measure distances, our results show that the situation is complicated by restrained dye orientations. Such dyes may be very useful in biomolecular FRET studies if the orientation of labels is known and controlled, or if you are trying to distinguish conformational states without directly measuring distances. On the other hand, the dependency of FRET on $\kappa^2$ that is accentuated with bifunctional dyes may be hard to overcome.

Physical Chemistry Chemical Physics Accepted Manuscript

## 5 Acknowledgments

The work has been partially supported by the Foundation for Polish Science with the International PhD Project MPD/2009-3/4.

## References


1 I. D. Sahu, R. M. McCarrick, K. R. Troxel, R. Zhang, H. J. Smith, M. M. Dunagan, M. S. Swartz, P. V. Rajan, B. M. Kroncke, C. R. Sanders and G. A. Lorigan, *Biochemistry*, 2013, **52**, 6627–6632.

2 R. M. Lsel, R. Philipp, T. Klai, K. Hideg and W. E. Trommer, *Bioconjugate Chemistry*, 1999, **10**, 578–582.

3 M. D. Wilcox, J. W. Parce, M. J. Thomas and D. S. Lyles, *Biochemistry*, 1990, **29**, 5734–5743.

4 M. R. Fleissner, M. D. Bridges, E. K. Brooks, D. Cascio, T. Kalai, K. Hideg and W. L. Hubbell, *Proc Natl Acad Sci U S A*, 2011, **108**, 16241–6.

5 B. Corry, A. C. Hurst, P. Pal, T. Nomura, P. Rigby and B. Martinac, *The Journal of General Physiology*, 2010, **136**, 483–494.

6 J. R. Lakowicz, *Principles of Fluorescence Spectroscopy*, Springer, 3rd edn, 2006.

7 Y. Wang, H. DeBerg, T. Nomura, M. Tonks-Hoffman, P. Rohde, B. Martinac and P. R. Selvin, *Biophysical Journal*, 2013, **104**, 385a.

8 C.-H. Ma, Y.-T. Liu, C. G. Savva, P. A. Rowley, B. Cannon, H.-F. Fan, R. Russell, A. Holzenburg and M. Jayaram, *Journal of Molecular Biology*, 2014, **426**, 793 – 815.

9 W. van der Meer, *Resonance Energy Transfer Theory and Data*, VCH, New York, 1994.

10 B. Corry, D. Jayatilaka, B. Martinac and P. Rigby, *Biophysical Journal*, 2006, **91**, 1032 – 1045.

11 R. E. Dale and J. Eisinger, *Proc. Natl. Acad. Sci. USA,*, 1976, **73**, 271–273.

12 M. Kampmann, C. E. Atkinson, A. L. Mattheyses and S. M. Simon, *Nat Struct Mol Biol*, 2011, **18**, 643 – 649.

13 J. M. Leeder and D. L. Andrews, *Proc. SPIE*, 2010, **7569**, 756922–756922–9.

14 J. Corrie, B. Brandmeier, J. Craik, V. Munasinghe, S. Howell, D. Trentham and J. Kendrickjones, *Biophysical journal*, 1997, **72**, 151 – 151.

15 T. Hirayama, S. Iyoshi, M. Taki, Y. Maeda and Y. Yamamoto, *Org. Biomol. Chem.*, 2007, **5**, 2040–2045.

16 L. Wu and K. Burgess, *J. Org. Chem.*, 2008, **73**, 8711–8718.

17 Y.-H. Ahn, J.-S. Lee and Y.-T. Chang, *Journal of the American Chemical Society*, 2007, **129**, 4510–4511.

18 B. Schuler, E. A. Lipman, P. J. Steinbach, M. Kumke and W. A. Eaton, *Proceedings of the National Academy of Sciences of the United States of America*, 2005, **102**, 2754–2759.

19 S. Doose, H. Neuweiler, H. Barsch and M. Sauer, *Proceedings of the National Academy of Sciences of the United States of America*, 2007, **104**, 17400–17405.

20 M. Hoefling, N. Lima, D. Haenni, C. A. M. Seidel, B. Schuler and H. Grubmüller, *PLOS ONE*, 2011, **6**, e19791.

21 L. Stryer, *Ann. Rev. Biochem*, 1978, **48**, 819–846.

22 J. C. Phillips, R. Braun, W. Wang, J. Gumbart, E. Tajkhorshid, E. Villa, C. Chipot, R. D. Skeel, L. Kalé and K. Schulten, *Journal of Computational Chemistry*, 2005, **26**, 1781–1802.

23 A. MacKerell, D. Bashford, M. Bellott, R. Dunbrack, J. Evanseck, M. Field, S. Fischer, J. Gao, H. Guo, S. Ha, D. Joseph-McCarthy, L. Kuchnir, K. Kuczera, F. Lau, C. Mattos, S. Michnick, T. Ngo, D. Nguyen, B. Prodhom, W. Reiher, B. Roux, M. Schlenkrich, J. Smith, R. Stote, J. Straub, M. Watanabe, J. Wiorkiewicz-Kuczera, D. Yin and M. Karplus, *Journal of Physical Chemistry B*, 1998, **102**, 3586–3616.

24 B. A. Corry and D. Jayatilaka, *Biophys. J.*, 2008, **133**, 2711–2721.

25 M. J. Frisch, G. W. Trucks, H. B. Schlegel, G. E. Scuseria, M. A. Robb, J. R. Cheeseman, G. Scalmani, V. Barone, B. Mennucci, G. A. Petersson, H. Nakatsuji, M. Caricato, X. Li, H. P. Hratchian, A. F. Izmaylov, J. Bloino, G. Zheng, J. L. Sonnenberg, M. Hada, M. Ehara, K. Toyota, R. Fukuda, J. Hasegawa, M. Ishida, T. Nakajima, Y. Honda, O. Kitao, H. Nakai, T. Vreven, J. A. Montgomery, Jr., J. E. Peralta, F. Ogliaro, M. Bearpark, J. J. Heyd, E. Brothers, K. N. Kudin, V. N. Staroverov, R. Kobayashi, J. Normand, K. Raghavachari, A. Rendell, J. C. Burant, S. S. Iyengar, J. Tomasi, M. Cossi, N. Rega, J. M. Millam, M. Klene, J. E. Knox, J. B. Cross, V. Bakken, C. Adamo, J. Jaramillo, R. Gomperts, R. E. Stratmann, O. Yazyev, A. J. Austin, R. Cammi, C. Pomelli, J. W. Ochterski, R. L. Martin, K. Morokuma, V. G. Zakrzewski, G. A. Voth, P. Salvador, J. J. Dannenberg, S. Dapprich, A. D. Daniels, . Farkas, J. B. Foresman, J. V. Ortiz, J. Cioslowski and D. J. Fox, *Gaussian 09 Revision D.01*, Gaussian Inc. Wallingford CT 2009.

26 A. Onufriev, D. Bashford and A. David, *The Journal of Physical Chemistry B*, 2000, **104**, 3712–3720.

27 A. Onufriev, D. Bashford and D. A. Case, *Proteins: Structure, Function, and Bioinformatics*, 2004, **55**, 383–394.

28 M. Hoefling and H. Grubmüller, *Computer Physics Communications*, 2013, **184**, 841 – 852.

29 K. Walczewska-Szewc and B. Corry, *Phys. Chem. Chem. Phys.*, 2014, **16**, 12317–12326.

30 P. R. Selvin and J. E. Hearst, *Proceedings of the National Academy of Sciences*, 1994, **91**, 10024–10028.

31 B. Corry, C. G. Cranfield and B. Martinac, in *Structure and Physiological Role of Ion Channels Studied by Fluorescence Spectroscopy*, John Wiley & Sons, Ltd, 2006, pp. 1–26.

32 P. R. Selvin, *Annual Review of Biophysics and Biomolecular Structure*, 2002, **31**, 275–302.

33 A. Hagan and T. Zuchner, *Analytical and Bioanalytical Chemistry*, 2011, **400**, 2847–2864.

34 K. Börjesson, S. Preus, A. H. El-Sagheer, T. Brown, B. Albinsson and L. M. Wilhelmsson, *Journal of the American Chemical Society*, 2009, **131**, 4288–4293.

35 F. D. Lewis, L. Zhang and X. Zuo, *Journal of the American Chemical Society*, 2005, **127**, 10002–10003.




This journal is © The Royal Society of Chemistry [year]

Physical Chemistry Chemical Physics Accepted Manuscript